

Article

Hydrothermal Carbonization as Sustainable Process for the Complete Upgrading of Orange Peel Waste into Value-Added Chemicals and Bio-Carbon Materials

Antonella Satira ^{1,2}, Emilia Paone ^{1,3,*}, Viviana Bressi ², Daniela Iannazzo ², Federica Marra ⁴, Paolo Salvatore Calabrò ¹, Francesco Mauriello ¹ and Claudia Espro ^{2,*}

¹ Dipartimento DICEAM, Università Mediterranea di Reggio Calabria, Loc. Feo di Vito, 89122 Reggio Calabria, Italy; antonella.satira@unirc.it (A.S.); paolo.calabro@unirc.it (P.S.C.); francesco.mauriello@unirc.it (F.M.)

² Dipartimento di Ingegneria, Università di Messina, Contrada di Dio—Vill. S. Agata, 98166 Messina, Italy; viviana.bressi@unime.it (V.B.); diannazzo@unime.it (D.I.)

³ Consorzio Interuniversitario per la Scienza e la Tecnologia dei Materiali (INSTM), 50121 Firenze, Italy

⁴ Dipartimento di Agraria, Università Mediterranea di Reggio Calabria, Loc. Feo di Vito, 89122 Reggio Calabria, Italy; fede.marra6@gmail.com

* Correspondence: emilia.paone@unirc.it (E.P.); espro@unime.it (C.E.)

Featured Application: Hydrothermal carbonization process can be efficiently used for the simultaneous production of value-added chemicals, including furans and levulinates, and carbon-based materials.



Citation: Satira, A.; Paone, E.; Bressi, V.; Iannazzo, D.; Marra, F.; Calabrò, P.S.; Mauriello, F.; Espro, C. Hydrothermal Carbonization as Sustainable Process for the Complete Upgrading of Orange Peel Waste into Value-Added Chemicals and Bio-Carbon Materials. *Appl. Sci.* **2021**, *11*, 10983. <https://doi.org/10.3390/app112210983>

Academic Editor: Luca Fiori

Received: 19 October 2021

Accepted: 17 November 2021

Published: 19 November 2021

Publisher's Note: MDPI stays neutral with regard to jurisdictional claims in published maps and institutional affiliations.



Copyright: © 2021 by the authors. Licensee MDPI, Basel, Switzerland. This article is an open access article distributed under the terms and conditions of the Creative Commons Attribution (CC BY) license (<https://creativecommons.org/licenses/by/4.0/>).

Abstract: In this study, a simple and green protocol to obtain hydrochar and high-added value products, mainly 5-hydroxymethylfurfural (5-HMF), furfural (FU), levulinic acid (LA) and alkyl levulinates, by using the hydrothermal carbonization (HTC) of orange peel waste (OPW) is presented. Process variables, such as reaction temperature (180–300 °C), reaction time (60–300 min), biomass:water ratio and initial pH were investigated in order to find the optimum conditions that maximize both the yields of solid hydrochar and 5-HMF and levulinates in the bio-oil. Data obtained evidence that the highest yield of hydrochar is obtained at a 210 °C reaction temperature, 180 min residence time, 6/1 w/w orange peel waste to water ratio and a 3.6 initial pH. The bio-products distribution strongly depends on the applied reaction conditions. Overall, 180 °C was found to be the best reaction temperature that maximizes the production of furfural and 5-HMF in the presence of pure water as a reaction medium.

Keywords: orange peel waste (OPW); hydrothermal carbonization; hydrochar; 5-hydroxymethylfurfural (5-HMF); furfural (FU); levulinic acid (LA)

1. Introduction

Citrus fruits are among the most cultivated and processed fruits worldwide, with an annual production of about 152 million tons [1]. The citrus processing industry generates huge amounts of residues mainly in the form of pulp and peels, with the latter accounting for almost 50% of the wet fruit mass [2]. With more than 50 million metric tons in 2020 [3], the juice industry alone generates a huge volume of orange peel waste (OPW) that requires suitable management, taking into consideration the high OPW biodegradability that causes its fast fermentation, which is often uncontrolled. Therefore, the direct disposal of this secondary product without previous proper processing, raises serious environmental issues and economic loss for the citrus industry since traditional disposal strategies, such as incineration or landfilling, are expensive and insufficient in terms of environmental protection and energy efficiency [4,5].

To date, several technological innovations have been proposed to manage the OPW, mainly aimed at converting the bio-waste into a valuable resource for the extraction of essential oil and the sustainable production of biogas, bioethanol and other biobased chemicals such as pectin, bioethanol and acids [6–9].

Moreover, innovative approaches, such as the catalytic upgrading and the extraction of bioactive compounds, leading to an ecofriendly production of active ingredients having applications in different sectors, have been proposed in the last years. Even if the valorization of agro-industrial wastes by the preparation of bioactive materials can be considered a sustainable methodology, other factors also need to be taken into account, including the extraction method, the employed reagents and solvents, general expense and employing the use of toxic chemicals with long time/energy-demanding procedures, poor selectivity, and large volumes of solvents [10]. Furthermore, considering that citrus processing wastes contain high amounts of moisture, there is a great interest in their use as feedstock for thermochemical processes as well [11]. The hydrothermal carbonization (HTC) is simply a thermochemical conversion process carried out in a water medium under autogenous pressure at a relatively mild temperature (180–300 °C) and represents a promising treatment technique for the wet lignocellulosic biomass waste since it permits overcoming the drawbacks of conventional thermochemical processes that require the use of dry feedstocks [11]. During the hydrothermal carbonization, biomass is dehydrated in-situ and processed into solid, liquid and non-condensable gaseous products. The distribution of products depends on the process conditions and on the feedstock used, but in general 50–80% of the original biomass is present in the solid product, 5–20% in the aqueous phase which contains inorganic and organic matter, and 2–5% in the gas phase which is mainly composed of CO₂ [12]. Hydrothermal methods are largely used in petroleum-based refineries and are getting more and more attention from both scientific and industrial researchers since their process parameters can be easily translated into modern biorefineries aimed at the upgrading of lignocellulosic residues and wastes [13]. With respect to other (bio)refinery processes, HT protocols present several advantages in terms of sustainability since they generally adopt mild reaction conditions (e.g., temperature and pressure) without any homogeneous or heterogeneous catalysts and in the presence of water as a green reaction solvent (used as such or in combination with simple aliphatic alcohols) [13].

The carbonaceous residue obtained by the HTC of the citrus processing waste is rich in oxygenated functional groups, making it a promising material in a wide range of applications, including pollutants adsorption [14], soil amendment [15], as fuel in energy applications [11] and as a low-cost material for capacitor and sensing applications, as recently reported by some of the authors [16–19].

Recently, bio carbon-based catalysts, obtained via the hydrothermal carbonization of the orange peel, have been also successfully adopted for acid treatments of the lignocellulosic biomass aimed at biodiesel production [20], together with platform molecules such as xylose, levulinic acid and its derivatives [21,22]. Aqueous and gas phases obtained during the HTC of orange peels and other citrus fruit wastes are generally considered as by-products and only a few studies on their use as resources of added value chemicals have been reported [23]. In this regard, it should be emphasized that the light bio-oil, obtained by extraction from the aqueous phase resulting from the hydrothermal carbonization of citrus wastes, consists mainly of aldehydes, phenols, ketones, acids, and some small molecules and heterocyclic compounds of potential interest, such as feedstocks for the synthesis of chemicals and liquid bio-fuels [24]. Therefore, the optimization of the process operating parameters of the HTC, to obtain simultaneously biocarbon materials and value-added products, could represent a valid approach aimed at minimizing the environmental and economic impact caused by the management of the agro-industrial waste. Among the considerable range of chemical building blocks that can be obtainable from citrus wastes, furfural (FU) and 5-hydroxymethylfurfural (HMF) have shown a great potential in replacing fossil-derived molecules in the synthesis of valuable chemicals—including levulinate derivatives—and pharmaceuticals [25].

In this paper, the effect of process variables on the hydrothermal carbonization (HTC) of the orange peel as industrial processing waste is investigated for both hydrochar and furan derivative (FU and 5-HMF) in the bio-oil liquid fraction, in order to optimize the yields to solid and liquid fractions. The exploration of the single-step hydrothermal treatment represents a promising example of the wet organic waste valorization to produce value-added products with high yields and, at the same time, to avoid potential and serious environmental issues arising from the citrus processing waste management and disposal. Particular attention was given to the peculiar chemical composition of the liquid fraction obtained from the HT process that is rich in components of absolute strategic interest for the chemical and pharmaceutical industry.

2. Materials and Methods

2.1. Raw Materials

The orange peels (OPW), obtained from an industry located in Sicily (Italy), were grounded to a particle size smaller than 2 mm and stored in a sealed plastic bag at $-20\text{ }^{\circ}\text{C}$ (in order to decrease the rate of degradation and the loss of volatile matter) and defrosted before their use in the experimental tests.

Acetic acid (CH_3COOH) $\geq 99.8\text{ }w/w\%$ and sulfuric acid (H_2SO_4) $95.0\text{--}97.0\text{ }w/w\%$ as well as other chemicals were purchased from Merk Life Science S.r.l.

2.2. HTC Experimental Procedure

In a typical run, a mixture of wet OPW and deionized water at the desired biomass to water ratio was ultrasonically agitated for 15 min at room temperature ($20\text{ }^{\circ}\text{C}$) and then transferred into a 300 mL stainless steel autoclave (series 4540 Parr Instrument Company, IL, USA) for HTC. Since the water to solid ratio has a significant effect on the reaction products, a series of experiments setting the L:S ration to 4:1, 6:1, 12:1 and 24:1 (w/w) were performed. For all the experiments, a fixed amount of water was used. Prior to reaction, residual air was removed from the sealed reactor by repeatedly pressurizing with nitrogen and venting to atmosphere. In a typical HTC test, the reaction mixture was heated under autogenous pressure up to the reaction temperature ($150\text{--}300\text{ }^{\circ}\text{C}$), at a heating rate of $5\text{ }^{\circ}\text{C min}^{-1}$ continuously monitored through a thermocouple placed into the autoclave and connected to the reactor controller within the whole. The residence time, after reaching the reaction temperature, was set at 30 min, 60 min, 180 min and 300 min, at a stirring speed of 600 rpm. After the HTC reaction, the autoclave was rapidly cooled at room temperature. Then, the HTC solid and liquid products were separated by vacuum filtration, with a Buchner funnel and filter paper. Afterwards, 40 mL of the obtained liquid aqueous product was extracted by 40 mL of diethyl ether in a separation funnel for carrying out the GC-MS analysis. A rotary evaporator was used for removing diethyl ether at $40\text{ }^{\circ}\text{C}$. Each extraction was performed twice (150 mL of diethyl ether). The remaining liquid was defined as light bio-oil in this study. Anhydrous sodium sulfate was used as a drying agent of the light bio-oil after the extraction. The obtained light bio-oil samples were hereafter named as L-HC T-t, where T denotes the reaction temperature ($^{\circ}\text{C}$) and t represents the time (min) of the HTC experiments.

The product yield was calculated using the following equation:

$$\text{product yield (\%)} = \frac{\text{mass of desired product (g)}}{\text{mass of initial wet OPW (g)}} \times 100 \quad (1)$$

The solid hydrochar was sequentially washed with warm distilled water and finally dried overnight under vacuum at $100\text{ }^{\circ}\text{C}$. The obtained hydrochar samples are hereafter named as S-HC T-t, where T denotes the reaction temperature ($^{\circ}\text{C}$) and t represents the time (min) of the HTC experiments.

The hydrochar samples, obtained in the experiments performed at different initial pH values at $180\text{ }^{\circ}\text{C}$ and 60 min, were designated as SA-HC1, SA-HC2, AA-HC1, AA-HC2 and AA-HC3, where the number represents the pH value theoretically calculated,

and the prefixes SA and AA refer respectively to sulfuric acid and acetic acid used as acidifying agents.

The mass yield of HC (MY) was calculated using the following equation:

$$\text{mass yield, wt \%} = \frac{M_{\text{Hydrochar, g(db)}}}{M_{\text{Feedstock, g(db)}}} \times 100 \quad (2)$$

It is well known that the relationship between temperature and time, defined and quantified by Overend and Chornet using the severity coefficient (R_0) based on the assumptions of first-order kinetics and Arrhenius temperature behavior of the aqueous pre-hydrolysis of Kraft pulping, greatly influences the physicochemical properties of the lignocellulosic substrates during subcritical and supercritical water treatments [26]. Therefore, the role of time and temperature on the HTC of OP was interpreted in terms of (R_0), expressed as

$$\log_{10} R_0 = \log_{10} \left[t \times \exp\left(\frac{T - T_0}{14.75}\right) \right] \quad (3)$$

where t is the time (min), T is the temperature ($^{\circ}\text{C}$), T_0 is the reference temperature generally set at 100°C . Assuming the overall reaction following first-order kinetics and Arrhenius relation of temperature, the empirical parameter ω is the fitted parameter, which in this and most other studies is assigned the value of 14.75 and equates to a reaction that doubles in reaction rate for every 10°C increase in temperature. The ω value in severity function Equation (3) was shown to be inversely proportional to activation energy, as expressed below (4):

$$\omega = \frac{T_f^2 R}{E_a} \quad (4)$$

where T_f is the temperature in the middle of the range of experimental conditions (floor temperature); R is the universal gas constant; E_a is the apparent activation energy.

2.3. Characterization

2.3.1. Characterization of the Bio-Oil Fraction

Products in the aqueous liquid phase as obtained after the separation of the solid carbonaceous fraction were quantified by using an off-line Shimadzu HPLC equipped with an Aminex HPX-87-H column using the following parameters: mobile phase $5\text{ mM H}_2\text{SO}_4$ at a speed flow of 0.6 mL min^{-1} and the oven-heated at 70°C . Every measurement was performed in 30–60 min [27].

The chemical content of the extracted light bio-oil was analyzed by using a GCMS-QP2010 system (Shimadzu, Japan) equipped with a split-splitless injector. A HP-5 weak polar capillary column, $30\text{ m} \times 0.25\text{ mm i.d.} \times 0.32\text{ }\mu\text{m}$ film thickness, was used for each GC analysis. The carrier gas was helium at a constant flow rate of 24.3 mL/min . For the setup of each system, $0.5\text{ }\mu\text{L}$ of the GC sample was injected in split mode, with a split ratio of 1:10 for the sample injection into the column. The oven temperature started at 40°C (held for 1 min) and then was increased to 300°C (maintained for 5 min), with a heating speed of 3°C/min . The mass spectrometer operated in electron ionization mode at 70 eV and mass spectra were obtained in a molecular mass range (m/z) of 40–660. The temperature of the transfer line was 250°C . Compound identification was performed by comparison with spectra obtained from the US National Institute of Standards and Technology (NIST) mass spectral library (ver. 11).

2.3.2. Characterization of the Hydrochar Fraction

Fourier transform infrared (FTIR) spectra were registered using a Perkin Elmer Spectrum 100 spectrometer, furnished with a common ATR sampling accessory. Spectra were recorded at room temperature from 4000 to 600 cm^{-1} and with a resolution of 4.0 cm^{-1} , without any earlier handling. The morphology of hydrochar samples was investigated using a Zeiss 1540XB FE SEM (Zeiss, Germany) instrument operating at 10 kV [28]. The

crystalline structure of synthesized materials was investigated using the X-ray powder diffraction (XRD) by means of a Bruker D8 Advance A 25 X-ray diffractometer operating at 40 kV and in the range 20–80° (2-theta), with an increasing rate of 0.01°/s and the recorded diffractograms were deconvolved via an OriginPro 2018 software. B.E.T. surface area and porosity of samples were evaluated by nitrogen adsorption and desorption isotherms carried out at 77 K by a Quantachrome® ASiQwin™ instrument (Anton Paar Companies, Graz, Austria). The thermal stability in the air of investigated hydrochar samples was evaluated by thermogravimetry (TGA) carried out with TA Instruments SDTQ 600 (balance sensitivity: 0.1 mg). Samples (~15 mg) were heated at 20 °C/min from 100 °C up to 1000 °C using a constant air flow rate (100 mL/min), after a preliminary sample stabilization for 30 min at 100 °C to remove the eventually adsorbed water [29]. The weight loss (%) was calculated.

3. Results and Discussion

3.1. Hydrochar Solid Fraction

3.1.1. Hydrochar Yields and Chemical-Structural Characteristics

In order to analyze separately the effect of reaction temperature and time on hydrochar yields, a series of experiments at fixed solid to water ratio were carried out [30]. After 60 min of reaction, the hydrochar yield rose with the reaction temperature from 18.8% at 180 °C up to a maximum of 30.4% at 300 °C (Figure 1). The reaction time provided less decomposition of biomass than the temperature. It can be assumed that for relatively short reaction times of 60 min and for low reaction temperatures, the conversion of the initial biomass is still at a germinal stage, as evidenced by the SEM analysis reported in Figure 1. On the other hand, after only 60 min of reaction, as the temperature increases the conversion process becomes significant, favoring the increase in hydrochar yield.

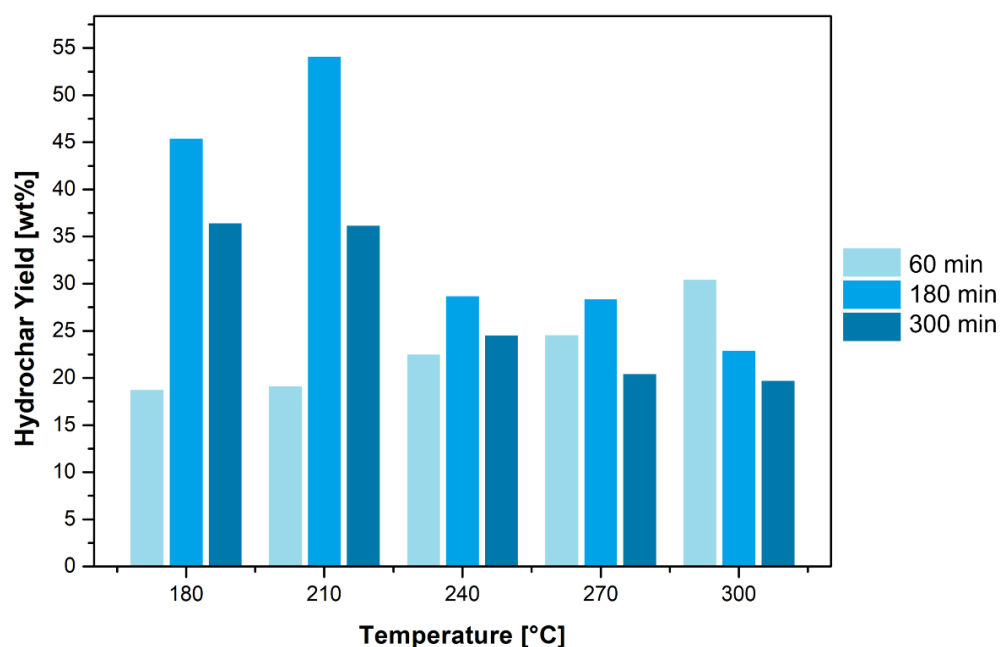


Figure 1. Hydrochar yield as a function of reaction temperature at a fixed reaction time.

After 180 min of reaction, the yield increases with the temperature from 45.4% at 180 °C up to the highest value of 54.1% at 210 °C. Such behavior is in line with the generally accepted reaction mechanism of the HTC process of lignocellulosic materials, where the cellulose degradation starts at a reaction temperature higher than 200 °C while, for a higher reaction temperature, a clear decrease in hydrochar yield is observed as a consequence of gas phase products formation. Accordingly, due to the more relevant volatilization processes under drastic conditions, a notable yield decrease is evident at longer reaction

times (300 min) already at 180 °C. Such findings, taking into account data obtained by other authors [30], confirm that process parameters (the reaction time and the reaction temperature) play a fundamental role on the hydrochar yields and cannot be analyzed separately. The reported results differ from those reported by Erdogan et al. [23] where a correlation between the reaction time and the hydrochar yield, in the HTC of the orange pomace in the T range 175–260 °C, was not found. This substantial difference is probably due to the distinctive content of cellulose and hemicellulose and their weight ratio, in the orange peel and in the pomace [31], that probably affects the global carbonization process with a consequent different amount of solid obtained over time, making the results between the two materials difficult to compare.

The simultaneous effect of temperature and reaction time, expressed in terms of $\log R_0$, on hydrochar yields is reported in Table 1. A substantial difference was observed in hydrochar yield produced at different $\log R_0$. Experimental data, also summarized in Table 1, indicate that a rise in the $\log R_0$ exerts a comparable promoting effect on the hydrochar production, resulting in a peculiar increasing trend with the severity coefficient and attaining a plateau of ca. 54.05 wt% at $\log R_0$ equal to 5.49 (210 °C at 180 min). A further increase of the $\log R_0$ causes a hydrochar yield decrease, with the lowest value of 19.69% found at the highest severity of 8.36 (300 °C at 300 min).

Table 1. Hydrochar yields as a function of $\log R_0$.

Sample	Log R_0	HC Yields (wt%)
S-HC ₁₅₀₋₆₀	3.25	13.27
S-HC ₁₈₀₋₆₀	4.13	18.74
S-HC ₁₈₀₋₁₈₀	4.61	35.37
S-HC ₁₈₀₋₃₀₀	4.83	36.40
S-HC ₂₁₀₋₆₀	5.01	49.10
S-HC ₂₁₀₋₁₈₀	5.49	54.05
S-HC ₂₁₀₋₃₀₀	5.71	36.13
S-HC ₂₄₀₋₆₀	5.90	29.45
S-HC ₂₄₀₋₁₈₀	6.37	28.66
S-HC ₂₄₀₋₃₀₀	6.59	24.48
S-HC ₂₇₀₋₆₀	6.78	24.53
S-HC ₂₇₀₋₁₈₀	7.26	22.34
S-HC ₂₇₀₋₃₀₀	7.48	20.39
S-HC ₃₀₀₋₆₀	7.66	20.40
S-HC ₃₀₀₋₁₈₀	8.14	20.87
S-HC ₃₀₀₋₃₀₀	8.36	19.69

A similar trend in the simultaneous effect of temperature and reaction time upon energy densification and mass yield have been reported by other researchers using different biomass raw materials [32–34], supporting that higher temperature and reaction time lead to an enrichment in fixed carbon and a consequent higher heat production but lower solids recovery, probably due to a higher conversion of cellulose, hemicellulose and lignin. This allows for a series of deoxygenating processes (e.g., dehydration, decarboxylation), resulting in the formation of organic matter and a decrease in oxygen and hydrogen content [31].

Termogravimetric (TGA) and energy-dispersive spectroscopy (EDS) analysis (shown in Figures S1 and S2 in ESI) of the different hydrochar samples, obtained under different hydrothermal temperatures at a fixed residence time of 180 min, confirm the noticeable role of reaction temperature in the yield and elemental composition of hydrochar. Apart from the S-HC₁₈₀₋₁₈₀ sample, the breakdown of all samples in the air's atmosphere takes place in three stages. Until 200 °C the weight loss (stage I) is very low (less than 2%), probably due to the hydrophobic nature of the hydrochars, which hinders the absorption of a large water quantity inside their structures. When increasing the temperature a large weight loss (stage II) starts, centered at around 300 °C and associated with the release

of organic volatile matters due to the decomposition of hemicellulose and cellulose. The successive stage (III) is related to surface and bulk hydrochar oxidation and suggests that the progressive loosing of the organic constituents, originally present in the orange peels, and the surface groups of hydrochar are formed at different hydrothermal temperatures, leading to samples production characterized by a different chemical composition.

Furthermore, EDS spectra of S-HC₂₁₀₋₆₀ reveals that at a lower temperature of reaction, many residual oxygenated groups still remain on the surface, evidenced by a high content of oxygen (about 20 wt%) and a lower content of carbon (ca. 78 wt%). On the contrary, an increasing of the reaction temperature up to 300 °C causes a decrease of the oxygen content (12.1%), ascribed to dehydration processes from cellulose to hydrochar [35] and a consequent enhancement of the carbon content (ca. 88 wt%).

As above mentioned, the reaction temperature influences not only the yields of the obtained hydrochar samples but also its morphology and composition, as revealed by SEM experiments. The morphology of samples prepared at lower hydrothermal temperature (Figure 2A) is not very dissimilar to that of the pectin and lignocellulose (the main components of the orange peels raw material) [36]. On the other hand, at 300 °C the material produced shows the presence of the characteristic hydrochar microspheres.

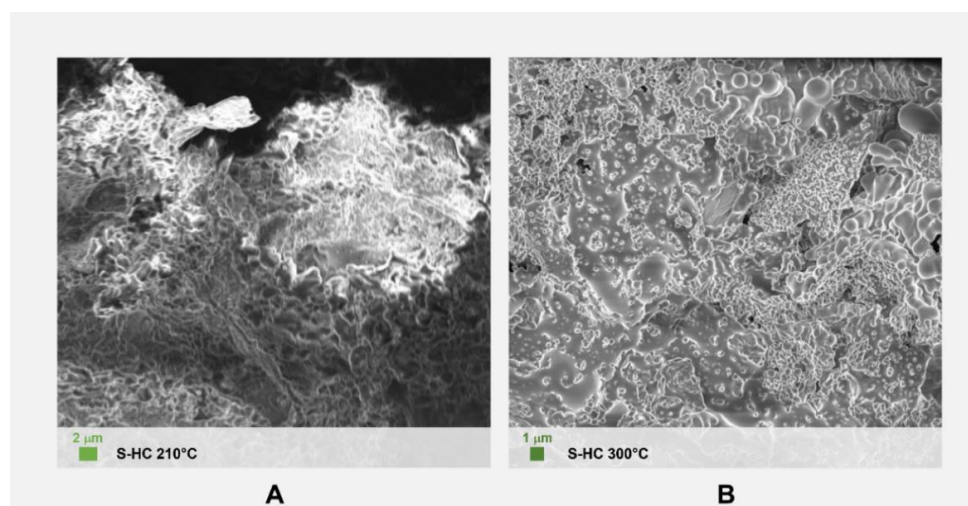


Figure 2. SEM analysis of (A) S-HC₂₁₀₋₆₀ and (B) S-HC₃₀₀₋₆₀.

XRD analysis was used for the determination of crystalline structures in the hydrochar samples (Figure 3).

The reflections of crystalline cellulose at 16 and 22.6 theta are noticeably evidenced in hydrochars obtained at the lowest temperature. As the temperature of the hydrochar preparation increases, a gradual shift from orderly crystallites to transition crystallites can be noticed in XRD spectra. Upon further increases of the hydrothermal temperature, these peaks disappear, whereas new broad peaks, at around 25 and 40 2-theta (*), related to turbostratic structure of disordered carbon coming from the (100) plane of graphite appear and gradually grow in intensity. Further increasing of the temperature to 300 °C leads to a complete conversion of the “crystalline stage” to the “amorphous stage”, as diffraction peaks at 300 °C suffer from broad shape, low intensities and low signal to noise ratio. As evidenced in Figure S3, the reaction time is irrelevant on the crystalline structure of the samples obtained at different reaction temperatures. This phenomenon can be explained by considering that the crystalline structure of cellulose in the lignocellulosic biomass has well-packed long chains characterized by strong hydrogen bonding networks, which maintain the sugar ring assembly promoted by the hydrolysis reaction occurring during the hydrothermal carbonization process [35].

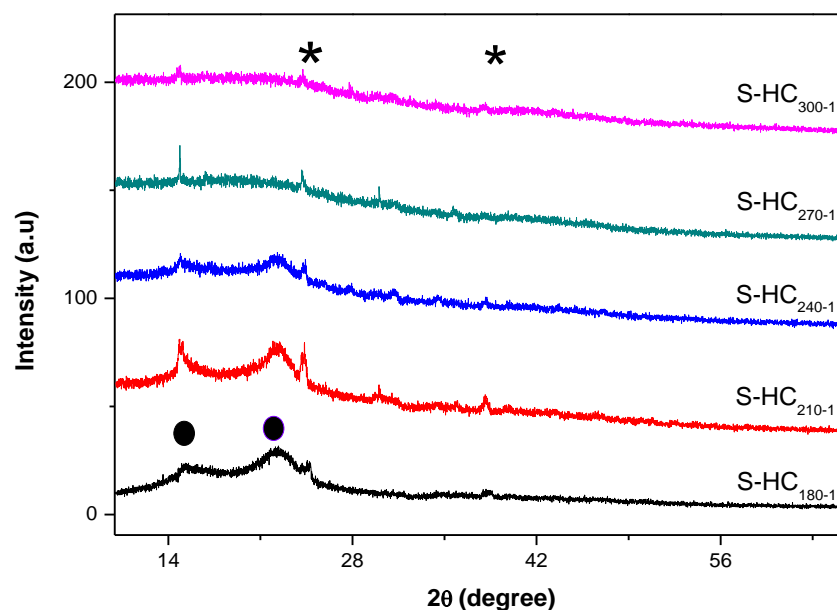


Figure 3. X-ray diffractograms of the hydrochar obtained at different temperatures after 60 min of reaction time. (● reflections of crystalline cellulose; * reflections of turbostratic structure of disordered carbon).

FTIR spectra at different reaction temperatures and reaction times are reported in Figure S4 in ESI. As can be seen from the FT-IR spectra, the reaction time does not affect the structural properties of the samples obtained at different reaction temperatures, therefore an example of a summary of the structural properties and N_2 adsorption-desorption isotherms obtained at various temperatures and at a fixed reaction time of 60 min is reported in Table 2. The adsorption bands at 1608 cm^{-1} and 1701 cm^{-1} correspond to the C=C vibrations and the C=O band, respectively, displaying the asymmetric stretch of aromatic rings, carbonyl, quinone, ester or carboxylic groups probably with a small quantity of amide, revealing the decarboxylation reaction and the aromatization of the orange peel waste during the hydrothermal process. The peaks at 1026 cm^{-1} can be attributed to the C–O stretching vibrations of carboxylic acids and esters or carbohydrates, while the band at about 3300 cm^{-1} suggests the O–H stretching of hydroxylic or carboxylic functionalities. Aliphatic C–H bands are found at $3000\text{--}2800\text{ cm}^{-1}$. The spectrum of S-HC₁₈₀₋₆₀ reveals a peak at $1120\text{--}1050\text{ cm}^{-1}$, possibly related to a C–O band of the lignocellulose component of the orange peels still present. According to XRD data, this peak decreases in intensity when increasing the treatment temperature. The presence of a peak at 1527 cm^{-1} strongly suggests the presence of a nitro-compound characterized by the N–O asymmetric stretching. The peak at 1431 cm^{-1} may also correspond to the asymmetric and symmetric stretching of the carboxylate (COO⁻) group. The fragment values became stronger and broader when experiments are carried out at a higher temperature, in agreement with TGA and EDS analysis confirming that during the HTC process a series of dehydration, decarboxylation and aromatization reactions occur, with a consequent decrease in the hydrochar yield as well as an enrichment in C content.

Moreover, the presence of an absorptions peak at 1026 cm^{-1} in the S-HC₁₈₀₋₆₀ sample, related to the C–O stretching vibration, can be again related to the presence of small amount of crystalline cellulose. As expected, upon increasing the reaction temperature, the absence of such a peak is indicative of the full conversion of OPW into biochar and bio-oil. Values of BET surface area and pore volume, reported in Table 2, relative to S-HC samples, at various temperatures and at a fixed reaction time of 60 min in accordance with other hydrochar prepared in similar experimental conditions [37] show that both parameters increase about three–four times when increasing the reaction temperature going from 180 to 300 °C.

Table 2. FTIR assignments and structural properties of the hydrochar samples at different reaction temperatures and a fixed reaction time of 60 min.

Observed Peak Intensity	Possible Functional Groups	Sample	B.E.T. S.A. (m ² /g)	Pore Volume (cc/g)	Pore Radius Dv(r) (Å)
3300 cm ⁻¹	O–H (alcohols, phenols, carboxylic acid)	S-HC ₁₈₀₋₆₀	4.9	0.009	17.9
3000 cm ⁻¹	C–H (aliphatic methyl)	S-HC ₂₁₀₋₆₀	5.5	0.008	20.4
1701 cm ⁻¹	C=O (ketone, aldehydes, amides)	S-HC ₂₄₀₋₆₀	7.7	0.010	17.6
1608 cm ⁻¹	C=C (aromatic rings, carbonyl, quinone, ester or carboxyl groups)	S-HC ₂₇₀₋₆₀	9.1	0.011	17.8
1527 cm ⁻¹	N–O (nitro)				
1431 cm ⁻¹	COO ⁻ (carboxylate)	S-HC ₃₀₀₋₆₀	18.4	0.029	22.4
1120 cm ⁻¹	C–O of lignocellulose				
1026 cm ⁻¹	C–O (carboxylic acid, esters)				

3.1.2. Effect of Initial pH and Solid to Water Ratio

Although the more relevant literature results identify reaction temperature and residence time as the main process parameters affecting the amount and chemical composition of the hydrochar produced, it is worth mentioning that both the solid to water ratio and the initial pH could play an important role, given that one of the goals of the HTC process is to break down the unbending structure of the starting biomass material into small and lower molecular weight chains. In fact, it is well known that addition of sulfuric acid or acetic acid in the reaction mixture can positively influence the HTC process by catalyzing hydrolysis reactions of cellulose and hemicellulose formed in the experimental conditions usually adopted. Regarding the effect of the initial pH, results reported in Table 3 show that the initial pH impacts the hydrochar yield, increasing as the higher acid concentration increases, with the highest yield of 30.12 wt% attained for SA-HC1, almost 50% higher than that observed in the reference experiment (180 °C, 60 min). However, these change slightly as the acetic acid concentration increases. Incidentally, we observe that CH₃COOH is a weak acid whereas H₂SO₄ is a strong acid when the first dissociation constant is concerned. Results also suggest that rather than the pH itself, it is the type of additive used that affects the yield. Indeed, the change in hydrochar yields could be explained considering that during the sulfuric acid catalyzed hydrolysis, insoluble humins indistinguishable from HC products are formed, with a subsequent enhancement of the number of solid products obtained.

Table 3. Hydrochar yields as a function of initial pH.

Sample	pH ¹	pH ²	Hydrochar Yield (wt%)
S-H ₁₈₀₋₆₀	-	3.60	18.74
SA-HC1	1	1.61	30.62
SA-HC2	2	1.89	27.36
AA-HC1	1	1.20	21.51
AA-HC2	2	1.80	19.39
AA-HC3	3	2.40	15.24

¹ theoretically calculated; ² experimentally measured.

On the contrary, the acetic acid is a natural by-product of HTC of lignocellulosic feedstocks, due to the hydrolysis and dehydration of cellulose and hemicellulose in the presence of subcritical water into short-chain organic acids: primarily acetic, formic, and lactic acid [38,39]. Therefore, a further addition of acetic acid in the reaction media, favoring the degradation of biomass components, leads to a higher heat production and a lower hydrochar yield.

Results obtained in this study (see Table S1 in ESI) also indicate that the role of the biomass/water ratio on hydrochar yield is insignificant for all values investigated. This finding is in agreement with the results reported by A. Toptas Tag et al. [40] for the HTC

of sunflower stalk as agricultural waste, poultry litter as animal waste, and algal biomass by Sapio et al. [41], but disagree with data reported by other authors [42,43]. In any case, in the literature there is no unanimous opinion on the role played by the different water/biomass ratio, and generally a fixed biomass to water ratio has been used by many authors. However, all results obtained as a function of the reaction temperature, reaction time, biomass/water ration and pH confirm that it is not always easy to make a direct comparison between the hydrochar yields reported in the literature and those reported in this study since there are many parameters that can affect the process, such as the experimental setup, the type of feedstock, the total solid and water amount, and the final amount of the hydrochar produced.

3.2. Hydrothermal Bio-Oil Liquid Fraction

3.2.1. Composition of Hydrothermal Bio-Oil Liquid Fraction

The general chemical composition of the light bio-oil obtained at different reaction temperatures and at a fixed residence time of 60 min was analyzed by GC-MS (Table 4).

Table 4. Major chemical components of the light bio-oil determined by GC-MS analysis.

Compounds Name	Sample				
	L-HC ₁₅₀₋₆₀	L-HC ₁₈₀₋₆₀	L-HC ₂₄₀₋₆₀	L-HC ₃₀₀₋₆₀	
	Peak Area%				
Furans	Furfural	18.94	16.69	1.63	-
	2-Furancarboxaldehyde, 5-methyl	14.86	7.88	5.05	-
	5-Hydroxymethylfurfural	41.97	61.82	28.61	-
Phenols	Phenol	0.57	0.10	4.72	9.62
	Catechol	0.60	0.29	4.52	8.64
	1,2-Benzenediol, 3-methyl	-	0.11	0.78	1.04
	Hydroquinone	-	-	1.91	7.26
	p-Cresol	-	-	0.79	2.17
	Phenol, 2-methyl	-	-	0.27	0.69
Acids	Benzoic acid	2.27	0.61	2.67	6.21
	2-Pentenoic acid	-	-	0.32	-
Ketones	2-Pentanone, 4-hydroxy-4-methyl	0.40	0.68	3.87	1.20
	Ethanone, 1-(2-furanyl)	0.69	0.46	0.40	1.86
	1,2-Cyclopentanedione, 3-methyl	0.63	0.81	-	-
	2-Cyclopenten-1-one, 2-hydroxy-3-methyl	-	-	4.37	0.99
	2-Cyclopenten-1-one, 2-methyl	-	-	0.61	5.83
	2-Cyclopenten-1-one, 3-methyl	-	-	0.61	7.41
Aldehydes	1H-Pyrrole-2-carboxaldehyde	0.86	0.41	0.66	-
	Benzaldehyde, 3-hydroxy	-	0.17	0.83	-
	Vanillin, acetate	-	-	1.07	-
Alcohols	α -Terpineol	0.91	0.24	-	1.01
	Benzyl alcohol	-	-	0.29	-
	3-Pyridinol	-	-	10.14	4.63
Alkenes	1-Nonadecene	0.24	0.33	1.65	-
	1-Pentadecene	-	0.59	3.51	-
	1-Heptadecene	-	-	3.64	-

The reaction mechanism involved in the formation of bio-oil during the HTC of various lignocellulosic biomasses has been described by several authors [38,44] and consists of a series of consecutive and parallel reactions starting with acid hydrolysis of polysaccharides to form monosaccharides. Glucose and fructose can be dehydrated by acids into 5-hydroxymethylfurfural and furfural. Furans and other reaction intermediates can

undergo further transformation processes (e.g., isomerization, condensation, rehydration, hydrations) or they can be degraded into humins [45].

As illustrated in Table 4, the light bio-oil is mainly divided into seven categories: furans, phenols, acids, ketones, aldehydes, alcohols and alkenes (Figure S5 in ESI). At lower HT temperatures, the main compounds at 200 °C are furan derivatives. When increasing the temperature, the composition of the light bio-oil becomes more complex, showing a higher concentration of acid phenolic compounds as a consequence of humins formation.

3.2.2. Production of Furan Derivatives and Levulinates from Hydrothermal Upgrading of Orange Peel Waste

To investigate the best reaction conditions that maximize the production of furan and levulinate derivatives, a systematic study on the effect of (i) time; (ii) temperature; (iii) initial acid concentration; and (iv) co-solvent was carried out.

Reaction temperature is surely a crucial parameter for investigating the overall productivity of furan derivatives starting from OPW. The yield profiles of FU, 5-HMF and levulinic acid are reported in Figure 4. Under neutral conditions, FU and 5-HMF yields gradually increase, reaching the highest value at 180 °C. The observed decrease in the production of furans at higher reaction temperatures is in line with other reports [46] and can be related to the formation of humin type by-products. Indeed, dark-brown insoluble products were formed in experiments carried out at 240 °C and 300 °C. As expected, under the reaction conditions adopted very low concentrations of levulinic acid (LA) were registered in all investigated reaction temperatures. A noticeable amount of LA can be seen at 300 °C due to the higher concentration of protons driving from the dissociation promoted by high reaction temperatures.

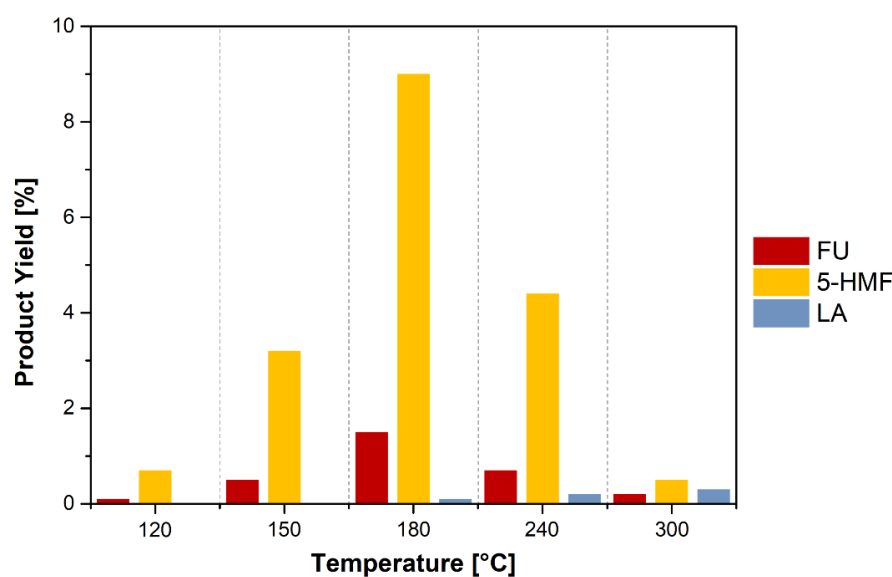


Figure 4. Effect of HTC reaction temperature on the production of furfural (FU), 5-hydroxymethylfurfural (5-HMF) and levulinic acid (LA) from OPW under neutral conditions (Reaction conditions: 20 g of OPW; 20 mL of H₂O; time: 60 min; autogenous pressure; stirring: 600 rpm).

Having found 180 °C as the best reaction temperature that maximizes FU derivatives, the conversion of OPW was also investigated at different reaction times (15, 30, 60, 180 and 300 min) (Figure 5). The highest 5-HMF and FU yields were already gained after only 30 min. A slight decrease in the production of furans was registered after 360 min and may be related both to the thermal degradation of furan derivatives as well as to the fact that a prolonged hydrolysis time increases formation of humins [47].

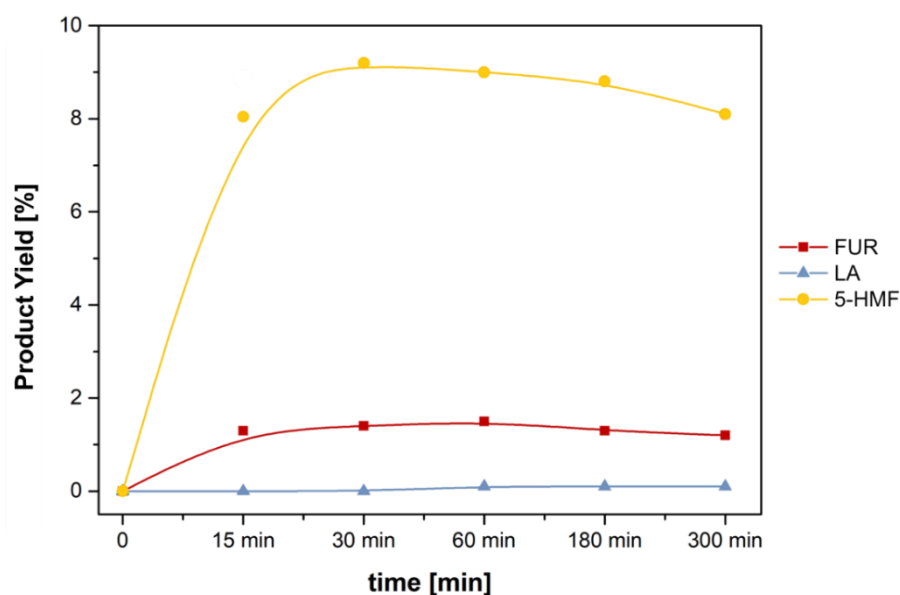


Figure 5. Effect of HTC reaction time on the production of furfural (FU), 5-hydroxymethylfurfural (5-HMF) and levulinic from (LA) OPW under neutral conditions (Reaction conditions: 20 g of OPW; 20 mL of H₂O; temperature: 180 °C; autogenous pressure; stirring: 600 rpm).

On the other hand, by changing the conditions using a sulfuric acid solution as reaction media, a decrease in the production of furans together with a higher production of levulinic acid is observed as a consequence of the acid hydrolysis (Figure 6). Upon increasing the H₂SO₄ content (from 0.2 to 1.0 M), a slight decrease in the overall LA can be noticed.

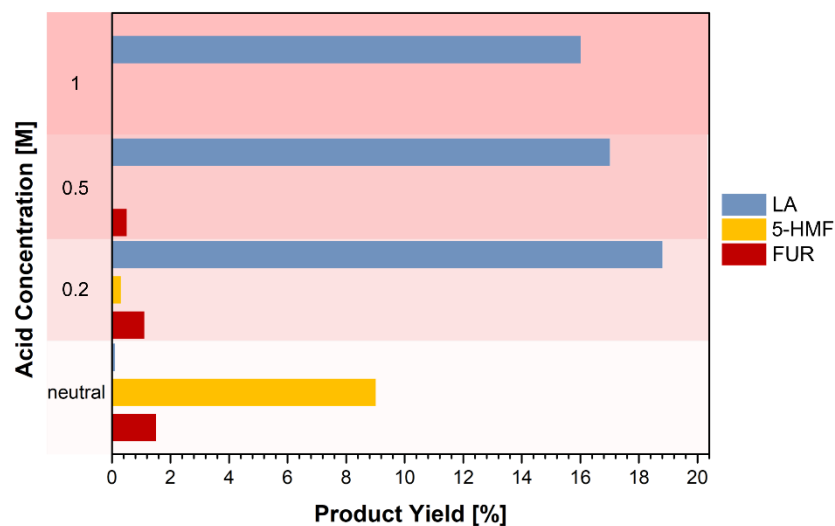


Figure 6. Effect of acid conditions on the production of furfural (FU), 5-hydroxymethylfurfural (5-HMF) and levulinic acid (LA) (Reaction conditions: 20 g of OPW; 20 mL solution of H₂SO₄ (from 0.1 to 1.0 M) in H₂O; temperature: 180 °C; time: 60 min; autogenous pressure; stirring: 600 rpm).

Analogous results are registered in the presence of simple alcohols as co-solvents, such as methanol and ethanol, that permit the direct formation of alkyl levulinates (Figure 7), used as flavoring/fragrance agents or as fuel bio-additives [48,49]. Moreover, methyl- and ethyl-levulinate now represent a valid starting bio-based feedstock for the preparation of γ -valerolactone [50,51] and find many applications ranging from flavoring agent to green solvent or as an intermediate in the synthesis of bio-based chemicals and polymers [52,53].

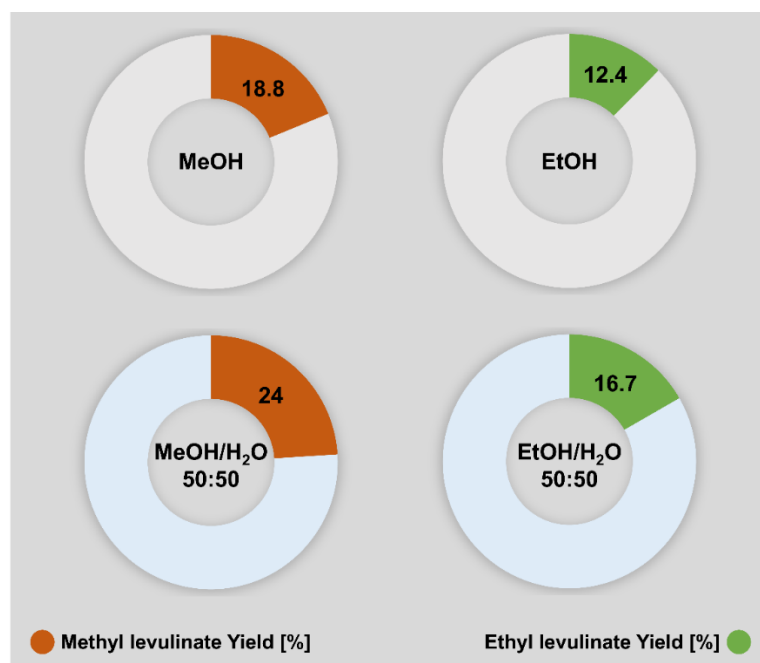


Figure 7. Co-solvent effect of HTC reaction temperature on the production of alkyl levulinates (Reaction conditions: 20 g of OPW; temperature: 180 °C; time: 60 min; autogenous pressure; stirring: 600 rpm).

Indeed, the best results in terms of alkyl-levulinate production were obtained when using a 0.2 M sulphuric acid solution with higher yields from the methanol esterification that, being characterized by a shorter carbon chain, is definitely a better entering group than ethanol (Table 5).

Table 5. Effect of acid conditions on the preparation of methyl-levulinate and ethyl-levulinate starting from OPW by using HTC process (Reaction conditions: 20 g of OPW; temperature: 180 °C; time: 60 min; autogenous pressure; stirring: 600 rpm).

Product	Solvent (wt:wt)	(0.1 M H ₂ SO ₄)	(0.1 M H ₂ SO ₄)	(0.1 M H ₂ SO ₄)
Methyl-levulinate	water: methanol (50:50)	7.1 (% yield)	24.0 (% yield)	14.2 (% yield)
Ethyl-levulinate	water: ethanol (50:50)	4.9 (% yield)	16.7 (% yield)	7.5 (% yield)

4. Conclusions

In this work, we demonstrated that the hydrothermal carbonization process can be successfully adopted for the complete upgrading of the orange peel waste into hydrochar and value-added chemicals. The main processing variables, reaction temperature, initial pH and residence time affect the mass yield (MY), while the solid to liquid ratio was found to be insignificant for all L/S investigated. Indeed, there was a strong correlation between temperature and residence time, suggesting that the role of these two variables cannot be analyzed independently. The highest yield of hydrochar was obtained at a 210 °C reaction temperature, 180 min residence time, 6/1 *w/w* orange peel waste to water ratio and a 3.6 initial pH. The results suggest that the conversion of the citrus waste occurs during the hydrothermal carbonization process due to a series of reactions such as decarboxylation and dehydration, leading to an improvement of the chemical, structural and morphological characteristics of the optimized hydrochar. This makes it a carbonaceous material suitable for a wide range of applications, both in the chemical and energy fields.

The bio-products distribution strongly depends on the applied reaction conditions. Overall, 180 °C was found to be the best reaction temperature that maximizes the production of furfural and 5-HMF in the presence of pure water as a reaction medium. On the other hand, by using a sulfuric acid solution as reaction media, levulinic acid can be easily obtained as a main product. Accordingly, a good production in methyl levulinate and ethyl levulinate can be achieved in the presence of methanol or ethanol, respectively, with the best yield obtained with methanol in the esterification reaction. Future research will be devoted to a prior recovery of more valuable compounds from OPW (e.g., limonene, pectin) before their hydrothermal conversion into hydrochar and bulk chemicals with a cascade high-to-low value approach.

Supplementary Materials: The following are available online at <https://www.mdpi.com/article/10.3390/app112210983/s1>. Figure S1. TGA curve in air of the hydrochar samples. Figure S2. SEM-EDS analyses of (a) S-HC₂₁₀₋₆₀ and (b) S-HC₃₀₀₋₆₀. The inset shows the elemental analysis of these samples. Figure S3. X-ray diffractograms of the hydrochar obtained at different temperature after (a) 180 min of reaction time and (b) 300 min of reaction time. Figure S4. FT-IR analysis of the hydrochar samples at (a) 60 min of reaction time; (b) 180 min of reaction time; (c) 300 min of reaction time. Table S1. Hydrochar yield as function of L/S ratio.

Author Contributions: Conceptualization: E.P. and C.E.; methodology: E.P., P.S.C., D.I., F.M. (Francesco Mauriello) and C.E.; formal analysis: A.S., V.B. and F.M. (Federica Marra); writing—original draft preparation: all authors; writing—review and editing: All authors have read and agreed to the published version of the manuscript.

Funding: This research received no external funding.

Institutional Review Board Statement: Not applicable.

Informed Consent Statement: Not applicable.

Data Availability Statement: The data presented in this study are available on request from the corresponding author.

Conflicts of Interest: The authors declare no conflict of interest.

References

1. FAO. *Fruit and Vegetables—Your Dietary Essentials. The International Year of Fruits and Vegetables*; FAO: Rome, Italy, 2021.
2. Choi, I.S.; Lee, Y.G.; Khanal, S.K.; Park, B.J.; Bae, H.J. A low-energy, cost-effective approach to fruit and citrus peel waste processing for bioethanol production. *Appl. Energy* **2015**, *140*, 65–74. [[CrossRef](#)]
3. FAS-USDA (Foreign Agricultural Service—United States Department of Agriculture). Citrus: World Markets and Trade. 2014. Available online: <https://apps.fas.usda.gov/psdonline/circulars/citrus.pdf> (accessed on 20 July 2020).
4. Satari, B.; Karimi, K. Citrus processing wastes: Environmental impacts, recent advances, and future perspectives in total valorization. *Resour. Conserv. Recycl.* **2018**, *129*, 153–167. [[CrossRef](#)]
5. Zema, D.A.; Calabrò, P.S.; Folino, A.; Tamburino, V.; Zappia, G.; Zimbone, S.M. Valorisation of citrus processing waste: A review. *Waste Manag.* **2018**, *80*, 252–273. [[CrossRef](#)]
6. Raimondo, M.; Caracciolo, F.; Cembalo, L.; Chinnici, G.; Pecorino, B.; D’Amico, M. Making virtue out of necessity: Managing the citrus waste supply chain for bioeconomy applications. *Sustainability* **2018**, *10*, 4821. [[CrossRef](#)]
7. De la Torre, I.; Martin-Dominguez, V.; Acedos, M.G.; Esteban, J.; Santos, V.E.; Ladero, M. Utilisation/upgrading of orange peel waste from a biological biorefinery perspective. *Appl. Microbiol. Biotechnol.* **2019**, *103*, 5975–5991. [[CrossRef](#)] [[PubMed](#)]
8. Fazzino, F.; Mauriello, F.; Paone, E.; Sidari, R.; Calabrò, P.S. Integral valorization of orange peel waste through optimized ensiling: Lactic acid and bioethanol production. *Chemosphere* **2021**, *271*, 129602. [[CrossRef](#)]
9. Fidalgo, A.; Ciriminna, R.; Carnaroglio, D.; Tamburino, A.; Cravotto, G.; Grillo, G.; Ilharco, L.M.; Pagliaro, M. Eco-friendly extraction of pectin and essential oils from orange and lemon peels. *ACS Sustain. Chem. Eng.* **2016**, *4*, 2243–2251. [[CrossRef](#)]
10. Espro, C.; Paone, E.; Mauriello, F.; Gotti, R.; Uliassi, E.; Bolognesi, M.L.; Rodriguez Padron, D.; Luque, R. Sustainable production of pharmaceutical, nutraceutical and bioactive compounds from biomass and waste. *Chem. Soc. Rev.* **2021**, *50*, 11191. [[CrossRef](#)] [[PubMed](#)]
11. Burguete, P.; Corma, A.; Hitzl, M.; Modrego, R.; Ponceb, E.; Renz, M. Fuel and chemicals from wet lignocellulosic biomass waste streams by hydrothermal carbonization. *Green Chem.* **2016**, *18*, 1051–1060. [[CrossRef](#)]
12. Fang, J.; Zhan, L.; Ok, Y.S.; Gao, B. Mini review of potential applications of hydrochar derived from hydrothermal carbonization of biomass. *J. Ind. Eng. Chem.* **2018**, *57*, 15–21. [[CrossRef](#)]

13. Satira, A.; Espro, C.; Paone, E.; Calabrò, P.S.; Pagliaro, M.; Ciriminna, R.; Mauriello, F. The limonene biorefinery: From extractive technologies to its catalytic upgrading into p-cymene. *Catalysts* **2021**, *11*, 387. [[CrossRef](#)]
14. Xiao, K.; Liu, H.; Li, Y.; Yang, G.; Wang, Y.; Yao, H. Excellent performance of porous carbon from urea-assisted hydrochar of orange peel for toluene and iodine adsorption. *Chem. Eng. J.* **2020**, *382*, 122997. [[CrossRef](#)]
15. Kalderis, D.; Papameletiou, G.; Kayan, B. Assessment of orange peel hydrochar as a soil amendment: Impact on clay soil physical properties and potential phytotoxicity. *Waste Biomass* **2019**, *10*, 3471–3484. [[CrossRef](#)]
16. Pistone, A.; Espro, C. Current trends on turning biomass wastes into carbon materials for electrochemical sensing and rechargeable battery applications. *Curr. Opin. Green Sustain. Chem.* **2020**, *26*, 100374–100381. [[CrossRef](#)]
17. Gou, H.; He, J.; Zhao, G.; Zhang, L.; Yang, C.; Rao, H. Porous nitrogen-doped carbon networks derived from orange peel for high-performance supercapacitors. *Ionics* **2019**, *25*, 4371–4380. [[CrossRef](#)]
18. Bressi, V.; Ferlazzo, A.; Iannazzo, D.; Espro, C. Graphene quantum dots by eco-friendly green synthesis for electrochemical sensing: Recent advances and future perspectives. *Nanomaterials* **2021**, *11*, 1120. [[CrossRef](#)]
19. Espro, C.; Satira, M.; Anajafi, M.K.; Iannazzo, D.; Neri, G. Orange peels-derived hydrochar for chemical sensing applications. *Sens. Actuators B Chem.* **2021**, *341*, 130016–130027. [[CrossRef](#)]
20. Lathiya, D.R.; Bhatt, D.V.; Maheria, K.C. Synthesis of sulfonated carbon catalyst from waste orange peel for cost effective biodiesel production. *Bioresour. Technol. Rep.* **2018**, *2*, 69–76. [[CrossRef](#)]
21. Singh, M.; Pandey, N.; Dwivedi, P.; Kumar, V.; Mishra, B.B. Production of xylose, levulinic acid, and lignin from spent aromatic biomass with a recyclable Brønsted acid synthesized from d-limonene as renewable feedstock from citrus waste. *Bioresour. Technol.* **2019**, *293*, 122105. [[CrossRef](#)]
22. Pileidis, F.D.; Tabassum, M.; Coutts, S.; Titiric, M.-M. Esterification of levulinic acid into ethyl levulinate catalysed by sulfonated hydrothermal carbons. *Chin. J. Catal.* **2014**, *35*, 929–936. [[CrossRef](#)]
23. Erdogan, E.; Atila, B.; Mumme, J.; Reza, M.T.; Toptas, A.; Elibol, M.; Yanik, J. Characterization of products from hydrothermal carbonization of orange pomace including anaerobic digestibility of process liquor. *Bioresour. Technol.* **2015**, *196*, 35–42. [[CrossRef](#)]
24. Aboagye, D.; Banadda, N.; Kiggundu, N.; Kabenge, I. Assessment of orange peel waste availability in Ghana and potential bio-oil yield using fast pyrolysis. *Renew. Sustain. Energy Rev.* **2017**, *70*, 814–821. [[CrossRef](#)]
25. Xu, C.; Paone, E.; Rodríguez-Padrón, D.; Luque, R.; Mauriello, F. Recent catalytic routes for the preparation and the upgrading of biomass derived furfural and 5-hydroxymethylfurfural. *Chem. Soc. Rev.* **2020**, *49*, 4273–4306. [[CrossRef](#)]
26. Overend, R.P.; Chornet, E. Fractionation of lignocellulosics by steam-aqueous pretreatments. *Philos. Trans. R. Soc. Lond. Ser. A Math. Phys. Sci.* **1987**, *321*, 523–536.
27. Gumina, B.; Espro, C.; Galvagno, S.; Pietropaolo, R.; Mauriello, F. Bioethanol production from unpretreated cellulose under neutral self-sustainable hydrolysis/hydrogenolysis conditions promoted by the heterogeneous Pd/Fe₃O₄ catalyst. *ACS Omega* **2019**, *4*, 352–357. [[CrossRef](#)] [[PubMed](#)]
28. Malara, A.; Paone, E.; Bonaccorsi, L.; Mauriello, F.; Macario, A.; Frontera, P. Pd/Fe₃O₄ nanofibers for the catalytic conversion of lignin-derived benzyl phenyl ether under transfer hydrogenolysis conditions. *Catalysts* **2020**, *10*, 20. [[CrossRef](#)]
29. Malara, A.; Paone, E.; Frontera, P.; Bonaccorsi, L.; Panzera, G.; Mauriello, F. Sustainable exploitation of coffee silverskin in water remediation. *Sustainability* **2018**, *10*, 3547. [[CrossRef](#)]
30. Zhuang, X.; Zhan, H.; Songa, Y.; He, C.; Huang, Y.; Yin, X.; Wu, C. Insights into the evolution of chemical structures in lignocellulose and non-lignocellulose biowastes during hydrothermal carbonization (HTC). *Fuel* **2019**, *236*, 960–974. [[CrossRef](#)]
31. Rivas-Cantu, R.C.; Jones, K.D.; Mills, P.L. A citrus waste-based biorefinery as a source of renewable energy: Technical advances and analysis of engineering challenges. *Waste Manag. Res.* **2013**, *31*, 413–420. [[CrossRef](#)] [[PubMed](#)]
32. Resa, M.T.; Yang, X.; Coronella, C.J.; Lin, H.; Hathwaik, U.; Shintani, D.; Neupane, B.P.; Miller, G.C. Hydrothermal carbonization (HTC) and pelletization of two arid land plants bagasse for energy densification. *ACS Sustain. Chem. Eng.* **2016**, *4*, 1106–1114.
33. Yan, W.; Perez, S.; Sheng, K. Upgrading fuel quality of moso bamboo via low temperature thermochemical treatments: Dry torrefaction and hydrothermal carbonization. *Fuel* **2017**, *196*, 473–480. [[CrossRef](#)]
34. Yao, Z.; Ma, X.; Lin, Y. Effects of hydrothermal treatment temperature and residence time on characteristics and combustion behaviors of green waste. *Appl. Therm. Eng.* **2016**, *104*, 678–686. [[CrossRef](#)]
35. Wang, S.; Dai, G.; Yang, H.; Luo, Z. Lignocellulosic biomass pyrolysis mechanism: A state-of-the-art review. *Prog. Energy Combust. Sci.* **2017**, *62*, 33–86. [[CrossRef](#)]
36. Cai, J.; Li, B.; Wang, J.; Zhao, M.; Zhang, K. Hydrothermal carbonization of tobacco stalk for fuel application. *Bioresour. Technol.* **2016**, *220*, 305–311. [[CrossRef](#)]
37. Sevilla, M.; Fuertes, A.B. Chemical and structural properties of carbonaceous products obtained by hydrothermal carbonization of saccharides. *Chem. Eur. J.* **2009**, *15*, 4195–4203. [[CrossRef](#)]
38. Reza, M.T.; Uddin, M.H.; Lynam, J.G.; Hoekman, S.K.; Coronella, C.J. Hydrothermal carbonization of loblolly pine: Reaction chemistry and water balance. *Biomass Convers. Biorefinery* **2014**, *4*, 311–321. [[CrossRef](#)]
39. Reza, M.T.; Rottler, E.; Herklotz, L.; Wirth, B. Hydrothermal carbonization (HTC) of wheat straw: Influence of feedwater pH prepared by acetic acid and potassium hydroxide. *Bioresour. Technol.* **2015**, *182*, 336–344. [[CrossRef](#)]
40. Tag, A.T.; Duman, G.; Yanik, J. Influences of feedstock type and process variables on hydrochar properties. *Bioresour. Technol.* **2018**, *250*, 337–344.

41. Sabio, E.; Álvarez-Murillo, A.; Román, S.; Ledesma, B. Conversion of tomato-peel waste into solid fuel by hydrothermal carbonization: Influence of the processing variables. *Waste Manag.* **2016**, *47*, 122–132. [[CrossRef](#)] [[PubMed](#)]
42. Volpe, M.; Fiori, L. From olive waste to solid biofuel through hydrothermal carbonization: The role of temperature and solid load on secondary char formation and hydrochar energy properties. *J. Anal. Appl. Pyrolysis* **2017**, *124*, 63–72. [[CrossRef](#)]
43. Borrero-López, A.M.; Fierro, V.; Jeder, A.; Ouederni, A.; Masson, E.; Celzard, A. High added-value products from the hydrothermal carbonization of olive stones. *Environ. Sci. Pollut. Res.* **2017**, *24*, 9859–9869. [[CrossRef](#)] [[PubMed](#)]
44. Wu, K.; Gao, Y.; Zhu, G.; Zhu, J.; Yuan, Q.; Chen, J.; Cai, M.; Feng, L. Characterization of dairy manure hydrochar and aqueous phase products generated by hydrothermal carbonization at different temperatures. *J. Anal. Appl. Pyrolysis* **2017**, *127*, 335–342. [[CrossRef](#)]
45. Chheda, J.N.; Román-Leshkov, Y.; Dumesic, J.A. Production of 5-hydroxymethylfurfural and furfural by dehydration of biomass-derived mono- and poly-saccharides. *Green Chem.* **2007**, *9*, 342–350. [[CrossRef](#)]
46. Puccini, M.; Licursi, D.; Stefanelli, E.; Vitolo, S.; Raspolli Galletti, A.M.; Heeres, H.J. Hydrothermal treatment of orange peel waste for the integrated production of furfural, levulinic acid and reactive hydrochar: Towards the application of the biorefinery concept. *Chem. Eng. Trans.* **2016**, *50*, 223–228.
47. Silva, J.F.L.; Pinto Mariano, A.; Filho, R.M. Less severe reaction conditions to produce levulinic acid with reduced humins formation at the expense of lower biomass conversion: Is it economically feasible? *Fuel Commun.* **2021**, *9*, 100029. [[CrossRef](#)]
48. Murat Sen, S.; Gürbüç, E.I.; Wettstein, S.G.; Martin Alonso, D.; Dumesic, J.A.; Maravelias, C.T. Production of butene oligomers as transportation fuels using butene for esterification of levulinic acid from lignocellulosic biomass: Process synthesis and techno-economic evaluation. *Green Chem.* **2012**, *14*, 3289–3294.
49. Bond, J.Q.; Martin Alonso, D.; Wang, D.; West, R.M.; Dumesic, J.A. Integrated catalytic conversion of gamma-valerolactone to liquid alkenes for transportation fuels. *Science* **2010**, *327*, 1110–1114. [[CrossRef](#)]
50. Tabanelli, T.; Paone, E.; Blair Vásquez, P.; Pietropaolo, R.; Cavani, F.; Mauriello, F. Transfer hydrogenation of methyl and ethyl levulinate promoted by a ZrO₂ catalyst: Comparison of batch vs continuous gas-flow conditions. *ACS Sustain. Chem. Eng.* **2019**, *7*, 9937–9947. [[CrossRef](#)]
51. Vásquez, P.B.; Tabanelli, T.; Monti, E.; Albonetti, S.; Dimitratos, N.; Cavani, F. Gas-phase catalytic transfer hydrogenation of alkyl levulinates with ethanol over ZrO₂. *ACS Sustain. Chem. Eng.* **2019**, *7*, 8317. [[CrossRef](#)]
52. Wright, W.R.H.; Palkovits, R. Development of heterogeneous catalysts for the conversion of levulinic acid to γ -valerolactone. *ChemSusChem* **2012**, *5*, 1657–1667. [[CrossRef](#)]
53. Omoruyi, U.; Page, S.; Hallett, J.; Miller, P.W. Homogeneous catalyzed reactions of levulinic acid: To γ -valerolactone and beyond. *ChemSusChem* **2016**, *9*, 2037–2047. [[CrossRef](#)]